# Formation mechanism and size features of multiple giant clusters in generic percolation processes

Yang Zhang, Wei Wei, Binghui Guo, Renquan Zhang, and Zhiming Zheng

# Formation mechanism and size features of multiple giant clusters in generic percolation processes

Yang Zhang, Wei Wei*, Binghui Guo, Renquan Zhang and Zhiming Zheng

*LMIB and School of mathematics and systems sciences,*

*Beihang University,*

*100191, Beijing, China*

*\*weiw@buaa.edu.cn*

## Abstract

Percolation is one of the most widely studied models in which a unique giant cluster emerges after the phase transition. Recently, a new phenomenon that multiple giant clusters are observed in so called BFW model has attracted much attention, and how multiple giant clusters could emerge in generic percolation processes on random networks will be concerned in this paper. By introducing the merging probability and inspecting the distinct mechanisms which contribute to the growth of largest clusters, a sufficient condition to generate multiple stable giant clusters is given. Based on the above results, the BFW model and a new multi-ER model given by us are analyzed, and the mechanism of multiple giant clusters of these two models is revealed. Furthermore, large fluctuations are observed in the size of multiple giant clusters in many models, but the sum size of all giant clusters exhibits self-averaging as that in the size of unique giant cluster in ordinary percolation. Besides, the growth modes of different giant clusters are discussed, and we find that the large fluctuations observed are mainly due to the stochastic behavior of the evolution in the critical window. For all the discussion above, numerical simulations on BFW model and multi-ER model are done, which strongly support our analysis. The investigation of merging probability and the growth mechanisms of largest clusters provides insight for the essence of multiple giant clusters in the percolation processes and can be instructive for modeling or analyzing real-world networks consisting of many large clusters.

**INTRODUCTION**

Percolation transition, which concerns the emergence of large-scale connectivity in lattices or networks, has been regarded as a fundamental model of phase transitions in statistical physics [1]. It has many applications in materials science, network robustness as well as epidemic spreading, and has been widely studied [2].

In percolation processes, links or nodes are selected and occupied gradually with time. A famous and well studied model of percolation is the Erdös-Rényi (ER) random graph [3], in which links are chosen uniformly in complete graph to be occupied. Erdös and Rényi [3] proved that as the ratio of the number of links and the number of nodes passes the critical point $t_c = 1/2$, the model undergoes a second-order transition and a unique giant cluster emerges. This kind of classical percolation is also observed in directed networks [4], correlated networks [5] and clustered networks [6], in which second-order transition and unique giant cluster are common characteristics.

By a simple modification of the rule to choose links in ER model, Achlioptas, D'Souza and Spencer showed that the percolation can be discontinuous, which was called explosive percolation [7]. This surprising result led to intensive research later, and the efforts on different topologies like scale-free networks [8, 9], 2D square lattice [10, 11] and Bethe lattice [12] were made, also the tricritical point [13] and the transport properties [14] were discussed. Besides the Achlioptas process, many new models such as cluster aggregation model [15–17], Gaussian model [18, 19], Hamiltonian approach [20] have been devised and studied, showing that discontinuous transition can be made when the evolution mechanism produces many clusters which are relatively large in the subcritical regime [21]. Although some numerical [22–25] and theoretical results [26] demonstrated that explosive percolation in the original Achlioptas processes is actually continuous in the mean-field limit, discontinuous transition indeed exists in other alternative models, e.g., the global competitive percolation process [27, 28].

On the other hand, a new kind of percolation with multiple giant clusters was also discovered and attracts our attention. The so called BFW model [29] was analyzed by Chen and D'Souza [30], which exhibits a strongly discontinuous percolation and two stable giant clusters coexisting after the transition. In an earlier paper, percolation with multiple giant clusters was also discussed in a process of aggregation with freezing [31]. According to the

2

analysis of Chen et al. [30], the key to formation and coexisting of multiple giant clusters in BFW model is the high probability of sampling internal-cluster links in the supercritical region, and any link which would lead to merging two giant clusters will be rejected. Later, the BFW model was further studied on the lattice by K. J. Schrenk et al. [32]. However, their discussion concentrated on the BFW model, for further understanding of how multiple giant clusters emerge and their properties, we should consider the mechanisms in general processes.

In this paper, we consider a class of generic percolation processes and its evolution mechanism. The merging probability between clusters is introduced, which can explicitly express the rule of different percolation models, and is the most important factor in learning the evolution of the processes. By analyzing the merging probability and distinct mechanisms in the evolution of largest clusters in one step, we found only the mechanism of joining largest clusters together prevents the formation of multiple giant clusters, and then a sufficient condition to generate multiple giant clusters is got as well as the condition to have them coexist stably later. Two percolation models with multiple giant clusters are discussed to support our analysis, including both discontinuous and continuous cases. Furthermore, we investigate the size of multiple giants, and contrary to the determinate size of unique giant cluster in ordinary percolation, large fluctuations are observed in each of multiple giant clusters among different realizations. However, the sum of all giant cluster size shows no fluctuation when the internal links in the system are not considered. Besides, in one realization, the different growth modes of multiple giant clusters are discussed, with which we can determine the sizes of giant clusters later in the process if their early behavior is known.


**MERGING PROBABILITY IN GENERIC PERCOLATION PROCESSES**


The widely studied bond percolation on random networks is considered here, in which the percolation processes can be generally expressed as follows. Start from $N$ nodes with all links between nodes unoccupied, then each step one unoccupied link is selected and occupied with some rules, the process continues until a given number of steps are reached. Let $T$ be the total number of occupied links at current step, and the time $t = T/N$. At any time $t$, every unoccupied link $(i, j)$ has an occupying probability $p_t(i, j)$ to be occupied, which is determined by the specific rule. For two connected clusters $A$, $B$, the *merging probability*

$P_t(A, B) = \sum_{i \in A, j \in B} p_t(i, j)$ gives the probability that $A$, $B$ are connected by a link at time $t$. Obviously, $P_t(A, B) = P_t(B, A)$, $P_t(A, A)$ represents the probability of occupying an internal link in $A$, and $\sum_{A,B,A \neq B} P_t(A, B)/2 + \sum_A P_t(A, A) = 1$.

For convenience, in this paper we consider three assumptions on the merging probability:

(1) For two links $(i, j)$ and $(i', j')$, $i, i' \in A, j, j' \in B$, $p_t(i, j) = p_t(i', j')$, i.e., links in the same cluster have the same probability to be occupied. Then, we denote $p_t(A, B) \equiv p_t(i, j)$, $i \in A, j \in B$, and $P_t(A, B) = s_A s_B p_t(A, B)$, if $A \neq B$;

(2) Denote $s_A$ the size of cluster $A$. $P_t(A, B) = P_t(A', B')$, if $s_A = s_{A'}, s_B = s_{B'}, A \neq B, A' \neq B'$, i.e., two pairs of clusters with the same sizes must have the same merging probability. Then, without confusion, we can use $P_t(s_A, s_B)$ instead of $P_t(A, B)$ when $A \neq B$;

(3) $p_t(A, B) \geq p_t(A', B)$, if $s_A \leq s_{A'}$, i.e., the probability to occupy a link between large clusters is not larger than that between small clusters. Thus, $P_t(A, B) \geq s_A/s_{A'} P_t(A', B)$, if $s_A \leq s_{A'}$.

There is a general class of percolation processes which satisfies these three assumptions, including all the models we mentioned above, such as ER model, Achlioptas processes and BFW model.

For example, in ER model, $P_t(A, B)$ is simply the fraction of the number of links connecting $A$ and $B$ in the total number of unoccupied links,

$$P_t^{ER}(A, B) = \frac{s_A s_B}{C_N^2 - tN} \approx \frac{2 s_A s_B}{N^2}. \tag{1}$$

Note that $P_t^{ER}(A, B)$ only depends on $s_A$, $s_B$.

In many other models, $P_t(A, B)$ is also associated with the cluster size distribution $n(s, t)$, which is the number of clusters of size $s$ per node at time $t$. For product rule in Achlioptas processes, for two given clusters $A$ and $B$,

$$P_t^{PR}(A, B) = \frac{4 s_A s_B}{N^2} \sum_{s_{A'} s_{B'} > s_A s_B} s_{A'} s_{B'} n(s_{A'}, t) n(s_{B'}, t), \tag{2}$$

in which $\frac{2 s_A s_B}{N^2}$ is the probability we choose a link between $A$ and $B$, and the sum term is the probability we choose a link between two clusters whose size product is larger than $s_A s_B$. If we choose both of these two links, by product rule, $A$, $B$ will be connected.

Besides $s_A$, $s_B$ and $n(s, t)$, $P_t(A, B)$ may be associated with other quantities such as the stage $k$ in BFW model, which we will discuss later.

To study a percolation model, the merging probability is very important in learning the evolution of the process and the nature of the transition.

4

## ANALYSIS ON THE EMERGENCE OF MULTIPLE GIANT CLUSTERS

### Growth mechanisms in the evolution of largest clusters

In order to study the emergence of multiple giant clusters, it is worth to consider the evolution of largest clusters in general processes first. In [27], whenever a single link is occupied, the evolution of the largest cluster $\mathbf{C_1}$ was classified into three mechanisms which are discussed respectively for the analysis of discontinuous percolation transitions. Here, we use a similar classification when the evolution of $\mathbf{C_1}$ and $\mathbf{C_2}$ are both considered, and identify five distinct mechanisms. How these mechanisms impact on the formation of multiple giant clusters will be learned. Just like in [27], all existing clusters are ranked by their sizes from large to small, and the $i_{th}$ largest one is denoted by $\mathbf{C_i}$ with its size $C_i = |\mathbf{C_i}|$, $C_1 \geq C_2 \geq \ldots \geq C_{v_{max}}$, $v_{max}$ represents the total number of existing clusters.

Then, as discussed in [27], for the evolution of $\mathbf{C_1}$ and $\mathbf{C_2}$, there are essentially five distinct mechanisms: (1) Direct growth of $\mathbf{C_1}$: $\mathbf{C_1}$ connects with a small cluster with size $C_i \leq C_1$(except $\mathbf{C_2}$), $\mathbf{C_1} + \mathbf{C_i} \to \mathbf{C_1}, i \geq 3$; (2) Overtaking of $\mathbf{C_1}$: two small clusters of size $C_i, C_j \leq C_1$ join together to form one which is larger than the current largest cluster, $\mathbf{C_i} + \mathbf{C_j} \to \mathbf{C_1}$, and the original $\mathbf{C_1}$ becomes new $\mathbf{C_2}$; (3) Direct growth of $\mathbf{C_2}$: $\mathbf{C_2} + \mathbf{C_i} \to \mathbf{C_2}$; (4) Overtaking of $\mathbf{C_2}$: $\mathbf{C_i} + \mathbf{C_j} \to \mathbf{C_2}$; (5) Merging of $\mathbf{C_1}$ and $\mathbf{C_2}$: $\mathbf{C_1} + \mathbf{C_2} \to \mathbf{C_1}$, $\mathbf{C_3}$ becomes the new $\mathbf{C_2}$, which makes $C_1$ increase most but $C_2$ have a decrease of $C_2 - C_3$. The doubling mechanism considered in [27] is already included in the above cases, as we permit $C_i = C_1$ for $i > 1$.

When studying the formation of multiple giant clusters, the size ratio $C_1/C_2$ is very important, since it will be finite through the critical point when multiple giant clusters exist, otherwise in the thermodynamic limit $C_1/C_2 \to \infty$ after the transition. Next we inspect how these mechanisms impact on the evolution of $C_1/C_2$ respectively. First, let's look at the two overtaking mechanisms. Let $C_1(t)$ denote the size of $\mathbf{C_1}$ at time $t$, $\Delta t = \frac{1}{N}$ is the time increased after occupying one link. For the overtaking of $\mathbf{C_1}$, both $C_1$ and $C_2$ increase, and $C_1(t + \Delta t) = C_i(t) + C_j(t)$, $C_2(t + \Delta t) = C_1(t)$. As $C_i(t), C_j(t) \leq C_1(t)$, whenever mechanism (2) happens, after this step we have $C_1 \leq 2C_2$. Thus, the overtaking of $\mathbf{C_1}$ always keeps $C_1/C_2 \leq 2$. For the overtaking of $\mathbf{C_2}$, it only contributes to the growth of the size $C_2$. Thus the overtaking of $\mathbf{C_2}$ always reduces $C_1/C_2$.

Then, we turn to the direct growth mechanisms. The direct growth of $\mathbf{C_1}$ increases $C_1/C_2$, but the direct growth of $\mathbf{C_2}$ decreases it. With the assumption that $P_t(C_2, C_i) \geq \frac{C_2}{C_1} P_t(C_1, C_i)$, we have $P_t(C_1, C_i)C_i/P_t(C_2, C_i)C_i \leq C_1/C_2$ for every $i \geq 3$. Thus, together in one step, these two direct growth mechanisms won't increase $C_1/C_2$ in expected. What's more, we note that $C_1/C_2$ increases at most 1 in one step of direct growth when $\mathbf{C_1}$ merges with $\mathbf{C_3}$. Since the probability that the direct growth of $\mathbf{C_1}$ occurs for successively infinite steps is zero, thus in any time interval $[t_0, t_1]$, with probability one the maximal number of successive steps of direct growth of $\mathbf{C_1}$ is some finite $k$. Then, in every successive $k + 1$ steps, the direct growth of $\mathbf{C_2}$ occurs at least once. When $C_1(t_0)/C_2(t_0) \leq k$, after every $k + 1$ steps $C_1/C_2 \leq k$ too, which means $C_1/C_2$ will stay finite.

For the merging of $\mathbf{C_1}$ and $\mathbf{C_2}$, $C_1(t + \Delta t)/C_2(t + \Delta t) \geq C_1(t)/C_2(t) + 1$ at least. What's more, the merging of $\mathbf{C_1}$ and $\mathbf{C_2}$ is against the overtaking of $\mathbf{C_1}$, as $C_1(t + \Delta t) \geq C_2(t + \Delta t) + C_3(t + \Delta t)$, which means the overtaking of $\mathbf{C_1}$ is invalid for at least one step next.

With the above discussion, we can give a description of the evolution of $C_1/C_2$ in ordinary percolation processes. As we know, the largest cluster becomes a giant through the critical point $t_c$. Let's consider the critical window $[t_c - \epsilon, t_c + \epsilon]$, $\epsilon \to 0$ as $N \to \infty$. Before $t_c - \epsilon$, $P_t(\mathbf{C_1}, \mathbf{C_2})$ is very small due to their small sizes, then the overtaking and direct growth mechanisms keep $C_1/C_2 \sim O(1)$. In the critical window, $P_t(\mathbf{C_1}, \mathbf{C_2})$ increases with the growth of $\mathbf{C_1}$ and $\mathbf{C_2}$, and the merging of $\mathbf{C_1}$ and $\mathbf{C_2}$ dominates the evolution, thus $C_1/C_2$ increases rapidly. Beyond the critical window, $\mathbf{C_1}$ is macroscopic but $\mathbf{C_2}$ has $o(N)$ size, thus only one giant cluster can emerge. Therefore, the merging of $\mathbf{C_1}$ and $\mathbf{C_2}$ is the only mechanism which largely increases $C_1/C_2$ and prevents the formation of two giant clusters. If we can control $P_t(\mathbf{C_1}, \mathbf{C_2})$ to make $C_1/C_2$ stay in $O(1)$ order through the critical window, then $\mathbf{C_2}$ may become a giant cluster along with $\mathbf{C_1}$ too.

**Condition of multiple stable giant clusters**

If the overtaking of $\mathbf{C_1}$ exists until $C_1$ becomes of $O(N)$ size, two giant clusters must emerge since $C_1/C_2 \leq 2$. Otherwise, it doesn't exist since sometime before the transition, and from then with merging probability $P_t(\mathbf{C_i}, \mathbf{C_j})$ the expected growth $\Delta C_1 = C_1(t + \Delta t) -$

$C_1(t)$ and $\Delta C_2 = C_2(t+\Delta t) - C_2(t)$ can be simply expressed as follows,

$$\Delta C_1 = \sum_{i\geq 3} P_t(\mathbf{C_1}, \mathbf{C_i})C_i(t) + P_t(\mathbf{C_1}, \mathbf{C_2})C_2(t),$$

$$\Delta C_2 = \sum_{i\geq 3} P_t(\mathbf{C_2}, \mathbf{C_i})C_i(t) - P_t(\mathbf{C_1}, \mathbf{C_2})(C_2(t) - C_3(t))$$

$$+ \sum_{\substack{i,j\geq 3, i\neq j \\ C_i + C_j > C_2}} P_t(\mathbf{C_i}, \mathbf{C_j})(C_i(t) + C_j(t) - C_2(t)). \qquad (3)$$

For $\Delta C_1$, the first term in right hand side stands for the direct growth of $\mathbf{C_1}$, and the second refers to merging of $\mathbf{C_1}$ and $\mathbf{C_2}$; for $\Delta C_2$, the first term stands for the direct growth of $\mathbf{C_2}$, the second also associates with merging of $\mathbf{C_1}$ and $\mathbf{C_2}$, and the third denotes the overtaking of $\mathbf{C_2}$.

In one step, when $C_1/C_2 \sim O(1)$, if $P_t(\mathbf{C_1}, \mathbf{C_2})C_2(t) \sim o(\Delta C_1)$, then in (3), $\Delta C_2 > 0$ and $\Delta C_1/\Delta C_2 \leq C_1/C_2$, the impact of the merging of $\mathbf{C_1}$ and $\mathbf{C_2}$ can be neglected. If this is satisfied in all the following steps, noting that at the beginning $C_1/C_2 \leq 2$ and according to our above analysis, $C_1/C_2$ will stay in $O(1)$ order, and $\mathbf{C_2}$ must grow to be a giant cluster.

Before the critical window, all clusters are very small including $\mathbf{C_1}$ and $\mathbf{C_2}$, the merging of $\mathbf{C_1}$ and $\mathbf{C_2}$ is indeed negligible. Thus the evolution in the critical window should be mainly considered. In second-order transitions, $(C_1(t_c + \epsilon) - C_1(t_c - \epsilon))/N = A\epsilon$ for some constant $A > 0$ as $\epsilon \to 0$, and in first-order transitions, $(C_1(t_c + \epsilon) - C_1(t_c - \epsilon))/N = A$ as $\epsilon \to 0$. Thus, in average $\Delta C_1$ is no less than $O(1)$ order in the critical window. So if $P_t(\mathbf{C_1}, \mathbf{C_2})C_2(t) \sim o(1)$, then $P_t(\mathbf{C_1}, \mathbf{C_2})C_2(t) \sim o(\Delta C_1)$. Combining with the discussion before, we obtain the sufficient condition to have two giant clusters as follows,

$$P_t(\mathbf{C_1}, \mathbf{C_2}) \sim o(1/C_2(t)). \qquad (4)$$

In fact, sometimes the above condition may be too strong, especially when $C_3 \sim O(C_1)$, as $C_1/C_2$ is still $O(1)$ after the merging of $\mathbf{C_1}$ and $\mathbf{C_2}$. Later, we have an example in which two giant clusters can also emerge for $P_t(\mathbf{C_1}, \mathbf{C_2}) \sim O(1/C_2(t))$ when $C_3 \sim O(C_1)$.

After two giant clusters $\mathbf{C_1}$ and $\mathbf{C_2}$ emerge in the system, they may merge together in a few steps, and ultimately only one can be observed. Thus we should consider the condition for two giant clusters to coexist stably. We call multiple giant clusters *stable* if with probability one they can coexist until any finite time $t$. This requires that, the probability that $\mathbf{C_1}$, $\mathbf{C_2}$ join together in a period of time $[t_c, t]$ is zero, which can be satisfied if

$$P_t(\mathbf{C_1}, \mathbf{C_2}) \sim o(1/N) \qquad (5)$$

in this period. Since after the transition, $C_2 \sim O(N)$, condition (5) coincides with condition (4).

The evolution of the first $k$ $(k = 3, 4, \ldots)$ largest clusters can be analyzed analogically, and if

$$\sum_{i,j \leq k, i < j} P_t(\mathbf{C_i}, \mathbf{C_j}) \sim o(1/C_k(t)), \tag{6}$$

the system will exhibit a percolation with $k$ stable giant clusters.

The fact that multiple giant clusters could emerge in our condition (6) seems amazing compared to ordinary percolation. Obviously, this is due to the controlling of merging probability. In ordinary percolation, all links are occupied uniformly and independently. However, in our condition the occupying probability of each link depends on the size of the merging clusters, which means the probability a link to be occupied can depend on the occupancy of other distant links. From the physical point of view, this implies nonlocal control. It is well known that including long-range correlations can give rise to important changes on the university class or even the nature of the transitions, especially in [33–35] the local cluster aggregation models, the nonlocal product rules and the percolation under pair-exclusion constraint have been studied respectively, all showing that strong nonlocal features make the transition change from ordinary to explosive percolation. Thus it is not surprising that in our condition a percolation model with the controlling of merging probability could have multiple giant clusters.

Next, we will study two models to support the above analysis. One is the already known BFW model, which has a discontinuous transition; the other is a *multi-ER model* constructed by us, through controlling merging probability of classical ER model, which has a continuous transition.

## MULTIPLE GIANT CLUSTERS IN BFW MODEL AND MULTI-ER MODEL

### Discontinuous percolation case: BFW model

In order to verify our analysis above, a well known BFW model which is initially introduced by Bohman, Frieze, and Wormald [29], is discussed here. It has been recently analyzed by Chen and D'Souza [30], showing a strongly discontinuous percolation with multiple stable giant clusters. The detailed rule of the BFW model is as follows.

Let $k$ denote the stage of the process, initially set $k = 2$, $u$ the total number of links sampled, $T$ the number of occupied links, $T = 0$ at the beginning as all the nodes are isolated. At each step $u$, one link $e_u$ is sampled from all unoccupied ones uniformly at random, and the following algorithm is implemented:

$l \leftarrow$ the maximum cluster size if $e_u$ is occupied

If $(l \geq k)$

   $\{$Occupy $e_u$, $u = u + 1$, $T = T + 1\}$

Else if $(T/u \geq g(k) = 1/2 + \sqrt{1/(2k)})$

   $\{u = u + 1\}$

Else

   $\{k = k + 1$ and repeat the algorithm$\}$.

The BFW model samples links uniformly from all the unoccupied ones, yet another process called restricted BFW (RBFW) is also considered in [30], in which the same rule is followed but only the links that connect distinct clusters (external links) can be sampled. The sizes of the largest and the second largest clusters per node in both BFW and RBFW processes are shown in Fig. 1(a). As discussed in [30], they both exhibit a strongly discontinuous transition at the same critical point $t_c = 0.976$, but after the transition, two stable giant clusters coexist in the BFW model while only one in the RBFW model.

Chen and D'Souza have carefully studied the mechanisms of the BFW model and showed that the high probability of sampling internal-cluster links in the supercritical region is the key to coexisting multiple giant clusters. In contrast, while internal links are forbidden to sample in RBFW model, no multiple giant clusters coexist then. Here we understand the mechanisms in our framework by considering the merging probability $P_t(A, B)$. From the above rule, if a link $e_u$ between two distinct clusters $A$, $B$ is sampled, then it is occupied in two cases:

(1) $s_A + s_B \leq k$, then occupation of $e_u$ won't lead to the largest cluster size $l > k$.

(2) $s_A + s_B > k$ but $T/u < g(s_A + s_B - 1)$, since $g(k) = 1/2 + \sqrt{1/(2k)}$ is a decreasing function, when $k \leq s_A + s_B - 1$, $T/u < g(k)$ and $k$ will increase until $k = s_A + s_B$ and $e_u$ is occupied.
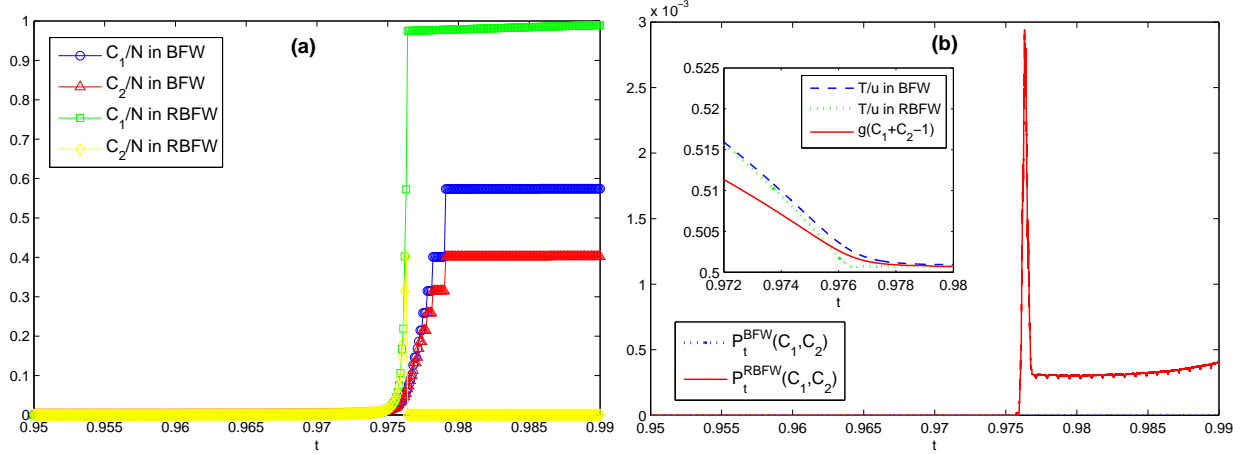
FIG. 1. (Color online) (a) $C_1/N, C_2/N$ versus time $t$ in BFW and RBFW model for $N = 10^6$, showing the emergence of two giant clusters in the BFW model after transition, while in the RBFW model the giant cluster is unique ultimately. (b) $P_t^{BFW}(C_1, C_2)$ (dotted blue line) and $P_t^{RBFW}(C_1, C_2)$ (red line) near $t_c$. Note that $P_t^{BFW}(C_1, C_2) = 0$ for all $t$. Inset, $T/u$ in both BFW and RBFW model are compared with $g(C_1 + C_2 - 1)$ near $t_c$. All data points are averages over 1000 realizations, $N = 10^6$.

We use $P_t(s_A, s_B)$ instead of $P_t(A, B)(A \neq B)$, and

$$P_t^{BFW}(s_A, s_B) = \begin{cases} s_A s_B / W, & \text{if } s_A + s_B \leq k \text{ or } T/u < g(s_A + s_B - 1). \\ 0, & \text{else.} \end{cases} \quad (7)$$

$W$ is a normalized constant, and denotes the total number of unoccupied links which are internal-cluster links or belong to the two cases. $P_t^{RBFW}(s_A, s_B)$ has the same expression as (7), but the number of internal-cluster links is not counted in $W$.

Obviously, $T/u$, the fraction of accepted links, is very important in determining the merging probability. In the BFW model, sampling internal-cluster links always increases $T/u$, as they are occupied for sure. In the subcritical region, all clusters are very small, and sampling internal-cluster links rarely occurs, thus the evolution of BFW and RBFW is similar. While in the supercritical region, when giant clusters emerge, there is a high probability to sample internal-cluster links in BFW model as discussed in [30], which makes $T/u$ always larger than $g(C_1 + C_2 - 1)$, and $P_t^{BFW}(C_1, C_2) > 0$. But this is not satisfied in RBFW model due to prohibiting sampling internal-cluster links.

We numerically get $T/u$, $k$ for every $t$ in both BFW and RBFW model, and calculate $P_t^{BFW}(C_1, C_2)$, $P_t^{RBFW}(C_1, C_2)$ by (7). Near $t_c$, the average over 1000 realizations is shown

in Fig.1(b). We can see that $P_t^{BFW}(C_1, C_2) = 0$ for all $t$, according to our analysis above, two giant clusters must emerge through the transition as we observed, and they will coexist stably in the later evolution. For RBFW model, in fact $C_2$ also grows to $O(N)$ size, but $P_t^{RBFW}(C_1, C_2) \gg 1/N$ for $t \geq t_c$ and has a peak at $t_c$, thus two giant clusters can't coexist stably, in a few steps two giants merge together with the largest jump in $C_1$ and no second giant cluster is left. Inset, near $t_c$, $T/u > g(C_1 + C_2 - 1)$ in BFW model while $T/u < g(C_1 + C_2 - 1)$ in RBFW model, which determines the difference between $P_t^{BFW}(C_1, C_2)$ and $P_t^{RBFW}(C_1, C_2)$.

The original BFW model can be generalized so that $g(k) = \alpha + \sqrt{1/(2k)}$, and parameter $\alpha$ controls the number of stable giant clusters. With decreasing $\alpha$, the transition is delayed and more giant clusters may appear since the merging probability of largest clusters gets more suppressed. For $\alpha = 0.3$, three giant clusters emerge at critical point $t_c^{0.3} = 0.998$, as shown in Fig. 2. We numerically calculate the merging probability between $\mathbf{C_1}$, $\mathbf{C_2}$ and $\mathbf{C_3}$ as well. Inset, we can see $P_t^{BFW}(C_2, C_3) = 0$ at all $t$ for $\alpha = 0.3$, in contrast, $P_t^{BFW}(C_2, C_3)$ has a peak at $t_c^{0.5}$ for $\alpha = 0.5$. Thus, there are only two giant clusters in BFW model with $\alpha = 0.5$, while three ones when $\alpha = 0.3$ as we observed.

### Continuous percolation case: multi-ER model

The well known ER model exhibits a second-order percolation transition, and a unique giant cluster emerges through the critical point $t_c = 0.5$. However, we can modify the ER model by controlling the merging probability to get multiple giant clusters. The way to control the merging probability is intuitive: when a link is randomly chosen like in ER model, it will not be occupied definitely, but only with probability $p$. $p$ may be different for different links, those links with smaller $p$ are more difficult to be occupied.

In our model, let $p = 1$ when it is an internal-cluster link, and $p = \exp(-\frac{\theta s_A s_B}{N^{4/3}})$ when the link connects two distinct clusters $A$, $B$, whose sizes are $s_A$, $s_B$ respectively. $N$ is the total number of nodes. $\theta \geq 0$ is a parameter which controls the number of giant clusters, obviously, if $\theta = 0$ it reduces to the original ER model. We call this *multi-ER model*.

We know before the critical window, all clusters have $o(N^{2/3})$ size in the ER model, and $C_1, C_2, \ldots, C_i \sim O(N^{\frac{2}{3}})$ for finite $i$ at $t_c = 0.5$ [36]. So $p$ is designed to make the early evolution same as the original ER model, but the merging probability between largest
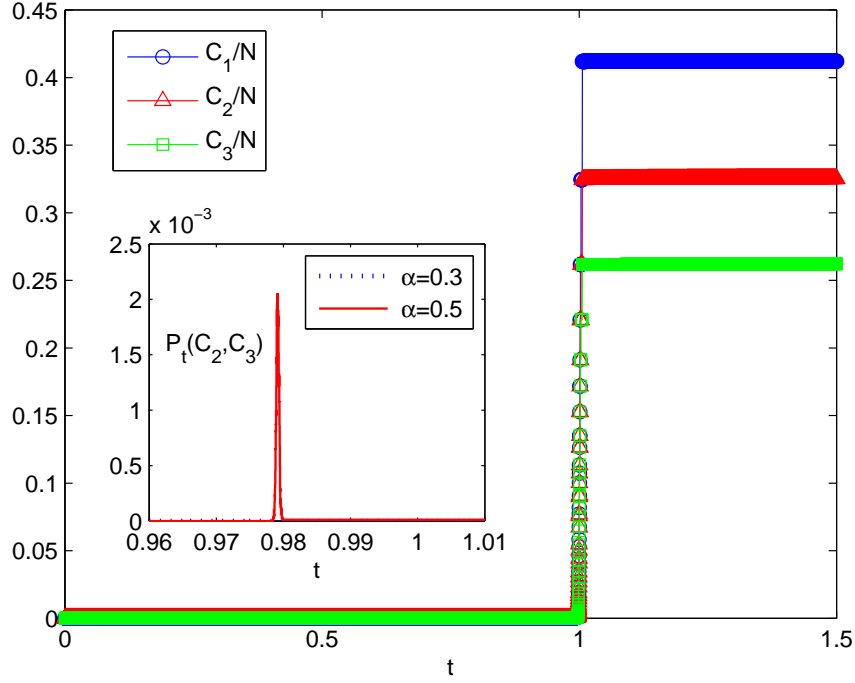
FIG. 2. (Color online) $C_1/N, C_2/N, C_3/N$ versus time $t$ in generalized BFW model with $\alpha = 0.3$ for $N = 10^6$. Inset, $P_t^{BFW}(C_2, C_3)$ for $\alpha = 0.3$ (dotted blue line) and $\alpha = 0.5$ (red line) near the critical point. $P_t^{BFW}(C_2, C_3) = 0$ at all $t$ for $\alpha = 0.3$.

clusters is controlled in the critical window.

We numerically implement our model for different $\theta$, and Fig. 3 shows $C_1/N$ for $\theta = 0$ and $C_1/N$, $C_2/N$ in a typical realization for $\theta = 1$. We can see, in contrast to original ER model ($\theta = 0$), two giant clusters emerge through the transition when $\theta = 1$, and they coexist stably.

From the definition, it is easy to get the merging probability as follows,

$$P_t(A, B) \sim \frac{2s_A s_B}{N^2} \exp(-\frac{\theta s_A s_B}{N^{4/3}}), \quad A \neq B. \tag{8}$$

$P_t(A, B)$ has a maximal point at $s_A s_B = N^{4/3}/\theta$, and decreases rapidly after across it. $max P_t(C_1, C_2) \sim O(1/C_2)$, but as $C_1$, $C_2$ grow, $P_t(C_1, C_2)$ decreases more rapidly than $1/C_2$. $P_t(C_1, C_2) \sim o(1/C_2)$ when $C_1 C_2/N^{4/3} \to \infty$.

In the critical window, the expected growth of $C_1$ and $C_2$ in one step can be estimated, when we get the cluster size distribution $n(s, t_c)$. In original ER model, we already know $n(s, t_c) \sim s^{-\frac{5}{2}}$ [37]. Since the same evolution before $t_c$, we infer that $n(s, t_c)$ should satisfy the
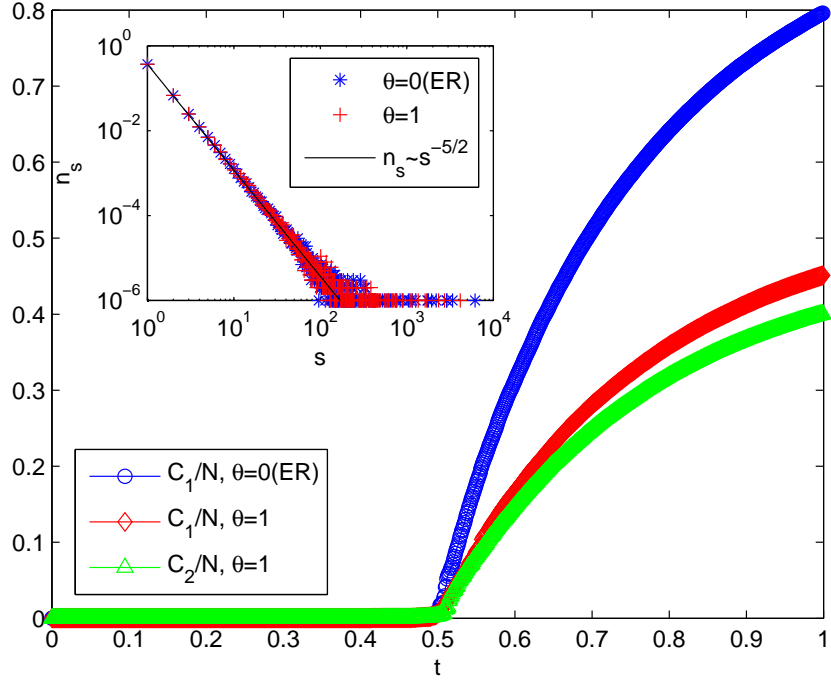
12

FIG. 3. (Color online) $C_1/N$ versus $t$ for $\theta = 0$ and $C_1/N$, $C_2/N$ versus $t$ in a typical realization for $\theta = 1$, $N = 10^6$. Inset, the cluster size distribution at $t_c = 0.5$, $n(s, t_c) \sim s^{-\frac{5}{2}}$ for both $\theta = 0$ and $\theta = 1$.

same power law in the multi-ER model. In the inset of Fig. 3, the cluster size distributions at $t_c$ for both $\theta = 0(\text{ER})$ and $\theta = 1$ are shown, which confirms this.

Thus, with (3) and (8) we have at $t_c$,

$$\Delta C_1 = \sum_{s=1}^{C_2} P_t(C_1, s) N n(s, t_c) s$$

$$\sim \int_{s=1}^{C_2} \frac{2C_1 s^{-\frac{1}{2}}}{N} \exp(-\frac{\theta C_1 s}{N^{4/3}}) ds$$

$$\geq \int_{s=1}^{C_2} \frac{2C_1 s^{-\frac{1}{2}}}{N} \exp(-\frac{\theta C_1 C_2}{N^{4/3}}) ds$$

$$\sim \frac{2C_1 \cdot 2(C_2^{\frac{1}{2}} - 1)}{N} \exp(-\frac{\theta C_1 C_2}{N^{4/3}}). \tag{9}$$

Analogically,

$$\Delta C_2 \sim \frac{2C_2 \cdot 2(C_3^{\frac{1}{2}} - 1)}{N} \exp(-\frac{\theta C_2 C_3}{N^{4/3}}) - \frac{2C_1 C_2(C_2 - C_3)}{N^2} \exp(-\frac{\theta C_1 C_2}{N^{4/3}})$$

$$= \frac{2C_2}{N^{2/3}} \exp(-\frac{\theta C_2 C_3}{N^{4/3}})[\frac{2(C_3^{\frac{1}{2}} - 1)}{N^{1/3}} - \frac{C_1(C_2 - C_3)}{N^{4/3}} \exp(-\frac{\theta C_2(C_1 - C_3)}{N^{4/3}})]. \tag{10}$$
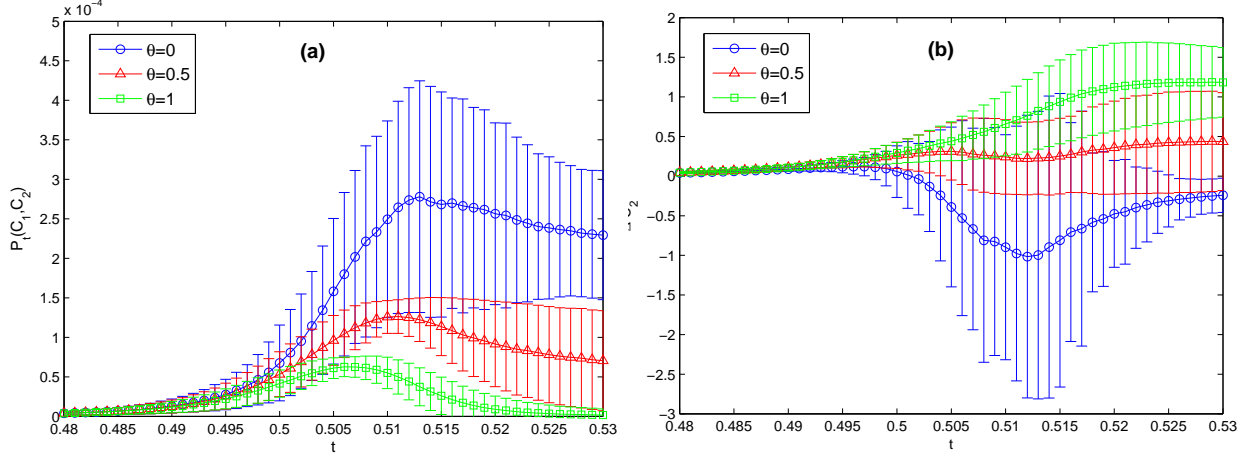
FIG. 4. (Color online) (a) The merging probability $P_t(C_1, C_2)$ and (b) the expected growth $\Delta C_2$ near the critical point for $\theta = 0, 0.5, 1$, $N = 10^6$. All data points are averaged over 1000 realizations; error bars indicate the standard deviations and reflect system-intrinsic fluctuations.

Note that $C_1, C_2, C_3 \sim O(N^{\frac{2}{3}})$ at $t_c$. For $\theta = 0$, $\Delta C_1 \sim O(1)$, which agrees with the fact that ER model has a second-order percolation transition at $t_c$. The direct growth term $\frac{2C_2 \cdot 2(C_3^{\frac{1}{2}} - 1)}{N}$ of $C_2$ is also $O(1)$, but as the the growing of $C_1$, $C_2$, the merging of $\mathbf{C_1}$ and $\mathbf{C_2}$ dominates the evolution and $\Delta C_2 < 0$, thus only one giant cluster can emerge through the transition.

For $\theta > 0$, we still have $\Delta C_1 \sim O(1)$, so the multi-ER model also exhibits a second-order transition at $t_c$. Pay attention to the last term in (10), we have $\frac{C_1(C_2 - C_3)}{N^{4/3}} \exp(-\frac{\theta C_2(C_1 - C_3)}{N^{4/3}}) \leq \frac{C_2(C_1 - C_3)}{N^{4/3}} \exp(-\frac{\theta C_2(C_1 - C_3)}{N^{4/3}}) \leq \frac{1}{\theta e}$, so for sufficiently large $\theta$, $\Delta C_2$ is positive and of $O(1)$ size throughout the critical window. That is to say, $\mathbf{C_2}$ will keep growing, when $C_1 C_2 \gg N^{4/3}$, $P_t(C_1, C_2) \sim o(1/C_2)$, then $\mathbf{C_2}$ will become a giant cluster like $\mathbf{C_1}$, as what we observed in Fig. 3 for $\theta = 1$.

We numerically verify the above analysis. $P_t(C_1, C_2)$ and $\Delta C_2$ are computed in 1000 realizations, and the averages are shown in Fig. 4 for $\theta = 0, 0.5, 1$. We can see, as $\theta$ increases, $P_t(C_1, C_2)$ is controlled to be smaller, making the merging of $\mathbf{C_1}$ and $\mathbf{C_2}$ be more strongly suppressed. Near $t_c$, $P_t(C_1, C_2)$ reaches its maximal point, and $max P_t(C_1, C_2) \sim O(N^{-2/3}) \sim O(1/C_2)$. But for $\theta = 1$, $P_t(C_1, C_2)$ decreases rapidly to nearly zero, and $P_t(C_1, C_2) \sim o(1/C_2)$ later. For $\Delta C_2$ it turns from negative to positive in the critical window as $\theta$ increases, and when $\theta = 1$, $\Delta C_2 > 0$ in the whole evolution.

We are aware that $P_t(C_1, C_2)$ and $\Delta C_2$ have large deviation due to the fluctuation of $C_1$,
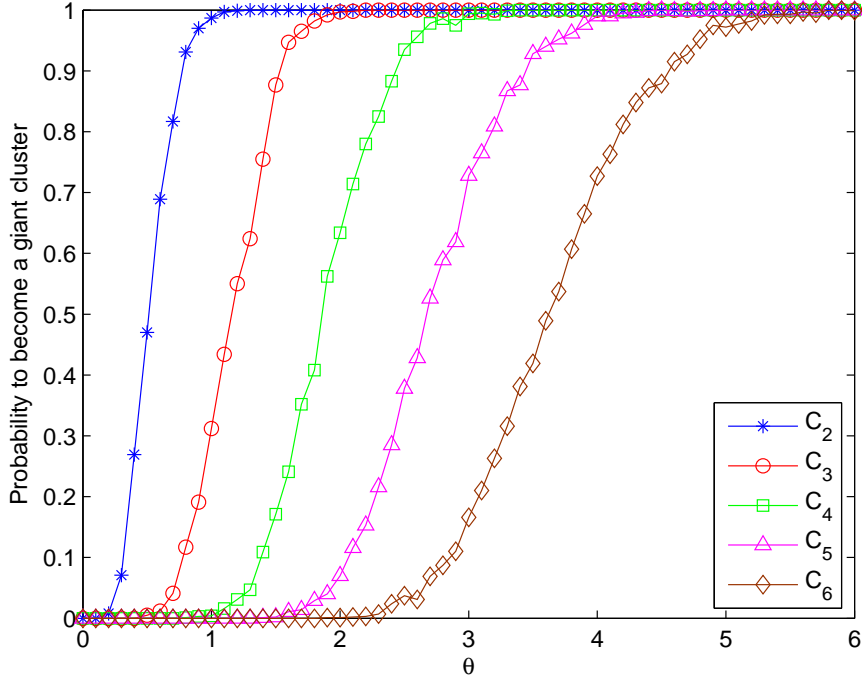
14

FIG. 5. (Color online) The proportion of realizations in which $C_i > 0.01N$ at $t = 1$, in total 1000 simulations versus $\theta$ for $i = 2, 3, 4, 5, 6$, $N = 10^6$.

$C_2$, $C_3$ near $t_c$ in different samples. This may lead to the uncertainty in the evolution of $C_2$ for some $\theta$. In Fig. 4, the average value of $\Delta C_2$ is near zero for $\theta = 0.5$, while the deviation of $\Delta C_2$ makes that whether it is positive is not determined. As a result, $\mathbf{C_2}$ will become a giant cluster in some realizations while not in others in this case.

Thus, for the cluster $\mathbf{C_2}$, there is an unstable parameter region, when $\theta$ belongs to the region (like $\theta = 0.5$), whether $\mathbf{C_2}$ becomes a giant cluster is not certain but with some probability. If $\theta$ is very small (like $\theta = 0$), $\mathbf{C_2}$ won't become a giant cluster, while for $\theta$ large enough (like $\theta = 1$), two giant clusters must emerge.

The discussion of $\mathbf{C_3}$, $\mathbf{C_4}$ and so on is analogical. Next, we numerically implement 1000 realizations for each $\theta$, and observe the evolution of $\mathbf{C_i}(i = 2, 3, 4, 5, 6)$. In practice, the process is continued until $t = 1$, and we regard $\mathbf{C_i}$ as a giant cluster if $C_i$ grows to larger than $0.01N$ in the realization. The proportion of realizations in which $C_i > 0.01N$ at $t = 1$ is shown in Fig. 5 versus $\theta$. We can see, as $\theta$ goes large, $\mathbf{C_i}$ starts to have probability to become a giant cluster, and the probability increases to one ultimately.

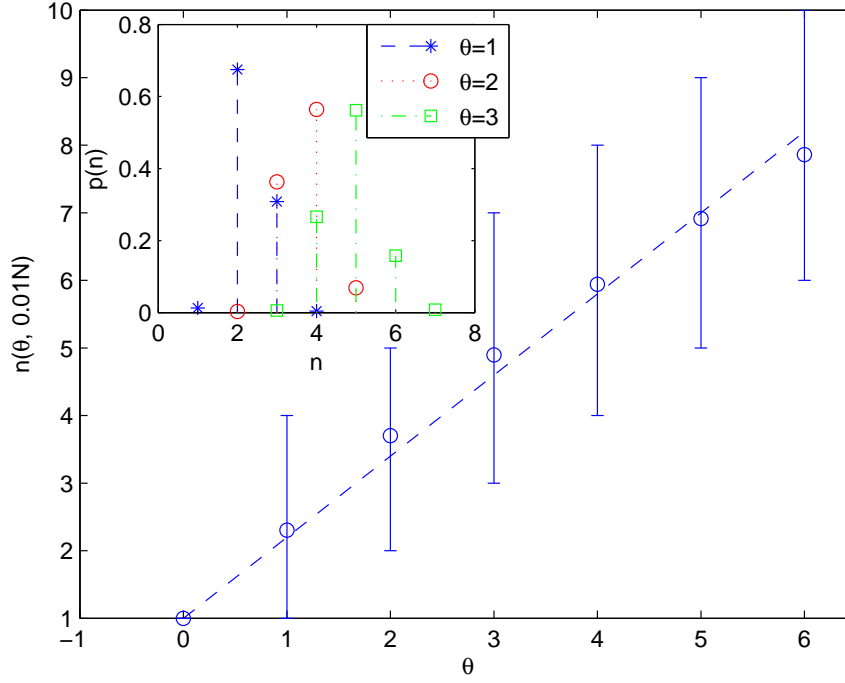On the other hand, for a given $\theta$, the number of stable giant clusters is not deterministic.

15

FIG. 6. (Color online) Number of stable giant clusters of size larger than $0.01N$ at $t = 1$ versus $\theta$, $N = 10^6$. The data points are averaged over 1000 realizations and dashed line is the best linear fit with $n = 1.2\theta + 1$. The lower and upper bars are minimum and maximum values respectively. Inset is the distribution of $n$ (number of stable giant clusters) for $\theta = 1, 2, 3$.

Denote $n(\theta, 0.01N)$ the number of stable giant clusters with size larger than $0.01N$ at $t = 1$. We implement 1000 independent realizations for $\theta = 0, 1, \ldots, 6$, the average, minimum and maximum values of $n(\theta, 0.01N)$ are shown in Fig. 6. The average of $n(\theta, 0.01N)$, denoted by $\overline{n}$, has an approximate linear relation with $\theta$. The dashed line is the best linear fitting with $\overline{n} = 1.2\theta + 1$.

## QUANTITATIVE ANALYSIS ON THE SIZE OF MULTIPLE GIANT CLUSTERS

### Fluctuation in the sizes of giant clusters

For ordinary percolation with unique giant cluster, it is well known that the order parameter, which refers to the relative size of the largest cluster $C_1(t)/N$, converges to a nonrandom function in the thermodynamic limit. That is to say, stochastic fluctuations can

be neglected as $N \to \infty$ [1]. Formally, this is called self-averaging.

However, when we study the size of multiple giant clusters, stochastic fluctuations are often observed in different realizations. In Fig. 7(a), $C_1/N$ and $C_2/N$ in three independent realizations of multi-ER model with $\theta = 1$ are shown, and clearly different realizations exhibit different behavior in the evolution, which implies large fluctuations exist in the size of giant clusters. This phenomenon is also observed in a modified BFW model with multiple giant clusters introduced by Chen and D'Souza [38], where the controlling function of BFW process is set to $g(k) = 1/2 + (2k)^{-\beta}$, and $\beta = 2$. Fig. 7(b) shows the size of giant clusters versus $t$ for three independent realizations of modified BFW model, similar as our multi-ER model, large fluctuations are found.

In order to learn it further, we consider the mean $\mu_1$ and the standard deviation $\chi_1$ of the largest cluster size $C_1/N$ at $t = 1$ for different $N$. If self-averaging holds for the process, then $\mu_1/\chi_1 \to 0$, as $N \to \infty$. In Fig. 8, $\mu_1$ and $\chi_1$ are numerically estimated based on $10^3$ runs for each $N$, and compared to ER model, $\mu_1/\chi_1$ does not tend to 0 as $N$ goes large for multi-ER and modified BFW. Thus, they are not self-averaging, large fluctuations observed are not due to finite size effect and don't disappear in the thermodynamic limit. Fig. 9 further illustrates the dependence of the mean and standard deviation on $N$ for both two models, the mean values of the largest two clusters seem to be stable for large $N$ and large standard deviations always exist for both.

The large random fluctuations in the order parameter of percolation have been discussed in [39], where two Achlioptas processes which are not self-averaging are introduced. According to their analysis, this may due to the "freezing in" of early variations, which means the microscopic fluctuations in the size of the largest component are magnified and propagated to later in the process. It is similar in percolation with multiple giant clusters. The behavior of the percolation process in the critical window is stochastic (For multi-ER model, the behavior is similar as ER model, where $C_1, C_2, \cdots$, is a random sequence which relates to a certain modified Brownian motion [40]). After the transition, the giant clusters have random initial sizes. Due to the condition we discussed above, it is known that the giant clusters won't join together in the subsequent evolution, thus they should grow respectively. However, there are usually some relations in the growth of different giant clusters which always hold for the later process, then the random size at the beginning will be propagated to later and lead to large fluctuations observed. The relations in the growth of different
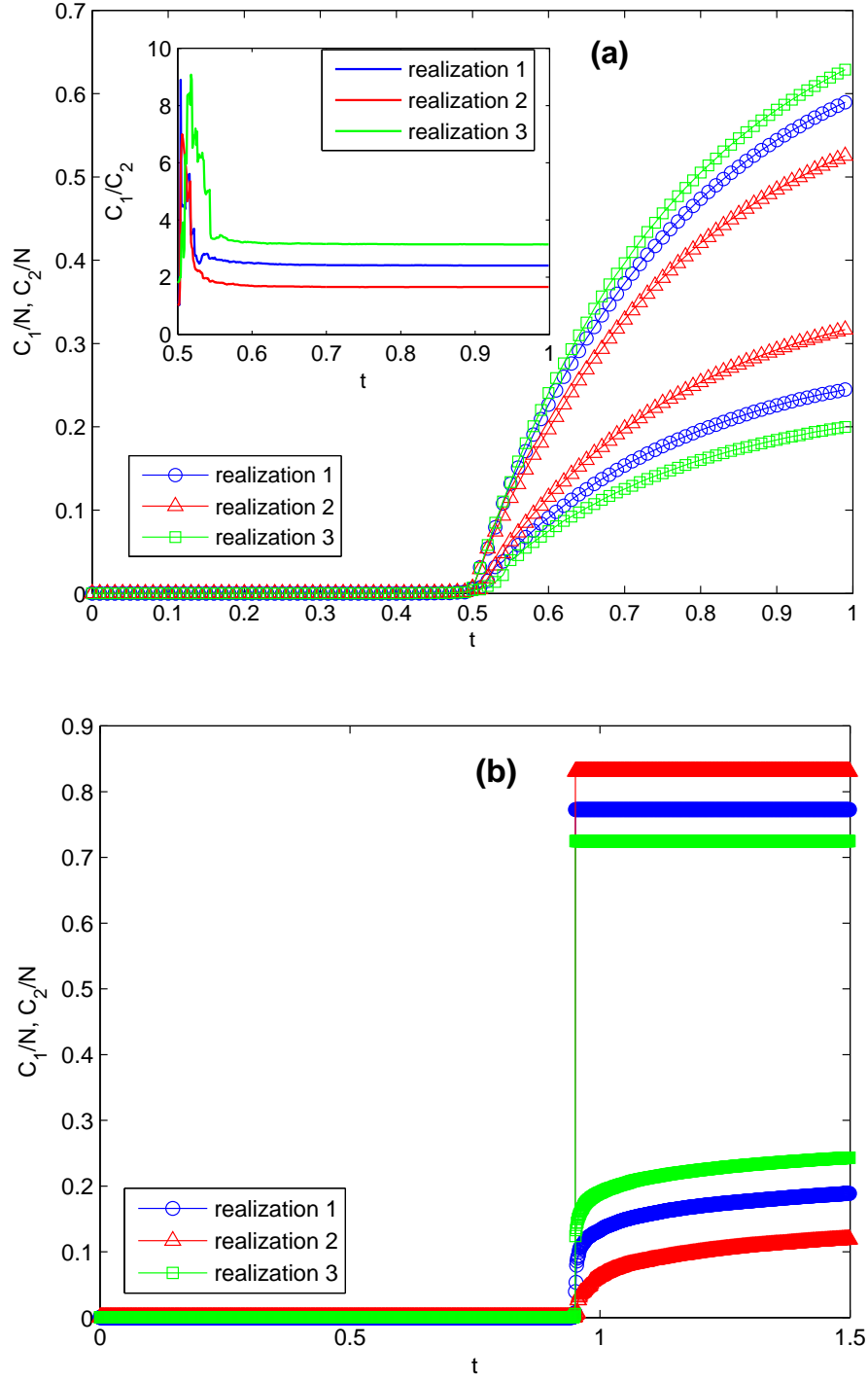
FIG. 7. (Color online) (a) $C_1/N, C_2/N$ versus $t$ in three independent realizations of multi-ER model with $\theta = 1$, $N = 10^6$. Inset, the ratios of the two giant clusters sizes $C_1/C_2$ after transition. (b) Three independent realizations of modified BFW model with $g(k) = 1/2 + (2k)^{-2}$, $N = 10^6$.
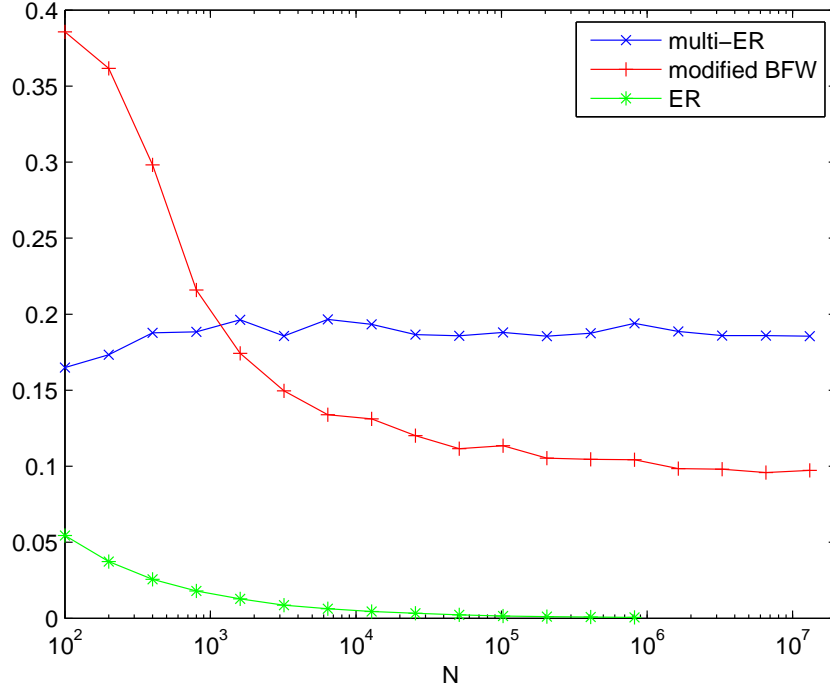
FIG. 8. (Color online) Estimated value $\mu_1/\chi_1$ of the order parameter $C_1/N$ at $t = 1$ versus $N$ (each based on $10^3$ realizations) for multi-ER, modified BFW and ER models.

giant clusters will be summarized as growth modes and discussed in detail later.

**The sum size of giant clusters**

Fig. 9 shows the mean and the standard deviation of the sum size of giant clusters $(C_1 + C_2)/N$. The fluctuations in the sum size are obviously smaller than the fluctuations in $C_1/N$, $C_2/N$ respectively, especially for the modified BFW model (the nondeterministic number of giant clusters in multi-ER model discussed in the previous section may be the reason which causes larger fluctuations).

The smaller fluctuations in the sum size imply that the sizes of two giant clusters $C_1/N$, $C_2/N$ are correlated, and their sum size may have a deterministic evolution in the process. Let's take multi-ER model as an example to study the evolution of the sum size of giant clusters. For simplicity, we suppose the system only has two giant clusters. After the transition, $P_t(C_1, C_2) \approx 0$ and the overtaking mechanisms don't work since other clusters are much smaller than $\mathbf{C_1}$, $\mathbf{C_2}$. By (3) we have $\Delta(C_1 + C_2) = \sum_{i \geq 3}[P_t(C_1, C_i) + P_t(C_2, C_i)]C_i$,
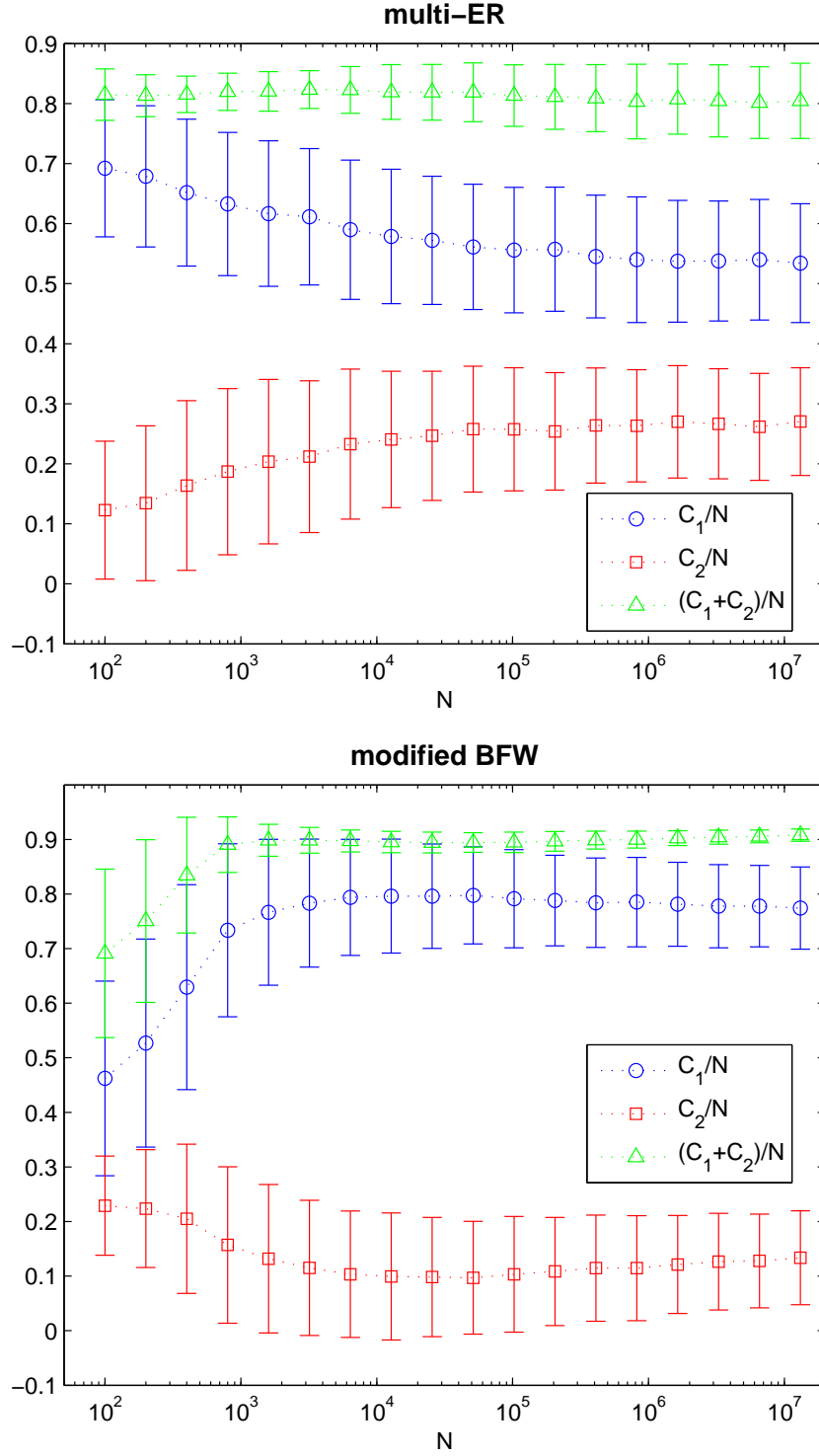
19

FIG. 9. (Color online) Simulation of the giant cluster size $C_1/N$, $C_2/N$ and the sum size $(C_1 + C_2)/N$ at $t = 1$ as a function of $N$ for the multi-ER and modified BFW models: mean and standard deviation (each based on $10^3$ realizations).

20

thus we can view $\mathbf{C_1}$ and $\mathbf{C_2}$ as one cluster, the evolution of which is very similar to that of the unique giant cluster with size $C_1 + C_2$ in original ER model. However, there is still one difference that the links between $\mathbf{C_1}$ and $\mathbf{C_2}$ won't be occupied while they may be occupied as internal links in the giant cluster for original ER model. We indicate that, the difference in occupying internal links is the only reason which leads to the small fluctuations in the sum size.

Denote $\widehat{L}$ the number of occupied external links, and $\hat{t} = \widehat{L}/N$, which is called noninternal time in [21]. If we consider the evolution of the sum size in noninternal time $\hat{t}$, then it must have no fluctuation in the thermodynamic limit and be self-averaging just as what's in the original ER model. To demonstrate our analysis, $(C_1 + C_2)/N$ versus $\hat{t}$ for the three different realizations of multi-ER model above are shown in Fig. 10(a), in which we can see a data collapse and no significant fluctuations. To learn it further, we calculate the standard deviation of the sum size of all giant clusters, denoted as $\chi_{sum}$, versus $\hat{t}$ over an ensemble of 1000 realizations, which is indeed very small and can be neglected beyond the threshold as shown in the inset.

Moreover, we can analytically fit the sum size versus $\hat{t}$ in multi-ER model since it has the same evolution as $C_1$ in original ER. For a classical ER network $A$ of $N$ nodes with mean degree $c$, the size per node $\gamma$ of the giant cluster is given by [37],

$$1 - \gamma = e^{-c\gamma}. \tag{11}$$

To calculate the number of external links per node $\hat{t}$ in this network, we divide $A$ into two parts: the giant cluster $G$ and the remaining network $B$. For $G$, there are $\gamma$ external links per node in it. For $B$, there is an important property that $B$ is still an ER network but with a smaller size $(1 - \gamma)N$ and a lower mean degree $c' < 1$ [40]. Obviously, $A$ and $B$ have the same number of isolated nodes, then with the Poisson degree distribution for ER network we have,

$$e^{-c}N = e^{-c'}(1 - \gamma)N. \tag{12}$$

The internal links in the remaining network $B$ can be neglected since the clusters in $B$ are very small and tree-like, which means all the $\frac{c'}{2}(1 - \gamma)N$ links in $B$ are external. The total number of external links in $A$ is the sum of two parts, thus,

$$\hat{t} = \frac{c'}{2}(1 - \gamma) + \gamma. \tag{13}$$

21

Combing (11), (12) and (13), $\gamma$ and $\hat{t}$ satisfy,

$$1 - \gamma = e^{-\frac{2(\hat{t}-\gamma)\gamma}{(1-\gamma)^2}}. \tag{14}$$

According to our analysis, the sum size in multi-ER model versus $\hat{t}$ must satisfy (14) too. Solving the self-consistent equation, we can give an analytical fit of the sum size, which coincides with $(C_1 + C_2)/N$ in the three realizations very well as shown in Fig. 10(a). This result further confirms that the sum size of giant clusters is self-averaging and has no fluctuation in noninternal time.

No fluctuation in the sum size of giant clusters seems to be a common feature in generic percolation processes with multiple stable giant clusters. For the original BFW model which doesn't show large fluctuations in the size of each giant cluster [30], the sum size does for sure. For the modified BFW model, things are similar as multi-ER. We realize that in noninternal time, the evolution of the sum size is just the same as $C_1$ in a modified RBFW model with $\beta = 2$. $(C_1 + C_2)/N$ versus $\hat{t}$ for the three different realizations of modified BFW model coincide with the simulation of RBFW model with $\beta = 2$, which is found in Fig. 10(b). Inset, the standard deviation over 1000 realizations is shown, which is neglectable except for at the critical point $t_c = 0.951$, thus $(C_1 + C_2)/N$ has no fluctuation beyond the transition. The large deviation at $t_c$ may due to the discontinuity of the transition [24].

Combining the results above, it is suggested that the sum size of all giant clusters plays a role of order parameter in the percolation with multiple giant clusters, as what $C_1/N$ does in the ordinary percolation.

**Different growth modes of giant clusters**

Besides the large fluctuation in the size of each giant cluster in different realizations, on the other hand, the relation of the growth of different giant clusters in one realization is discussed here. We still only consider the two giant clusters case. As the discussion above, for the evolution of giant clusters $\mathbf{C_1}$ and $\mathbf{C_2}$, only the direct growth mechanisms work. When considering the growth of these two giant clusters, the discussion can be classified into three modes in general.

Mode 1. $\Delta C_1/\Delta C_2 = C_1/C_2$. As in multi-ER model, $P_t(C_1, C_i) \sim \frac{2C_1 C_i}{N^2}$, $P_t(C_2, C_i) \sim \frac{2C_2 C_i}{N^2}$ since $C_i$ is very small, then $P_t(C_1, C_i)/P_t(C_2, C_i) = C_1/C_2$ for every $i \geq 3$ and
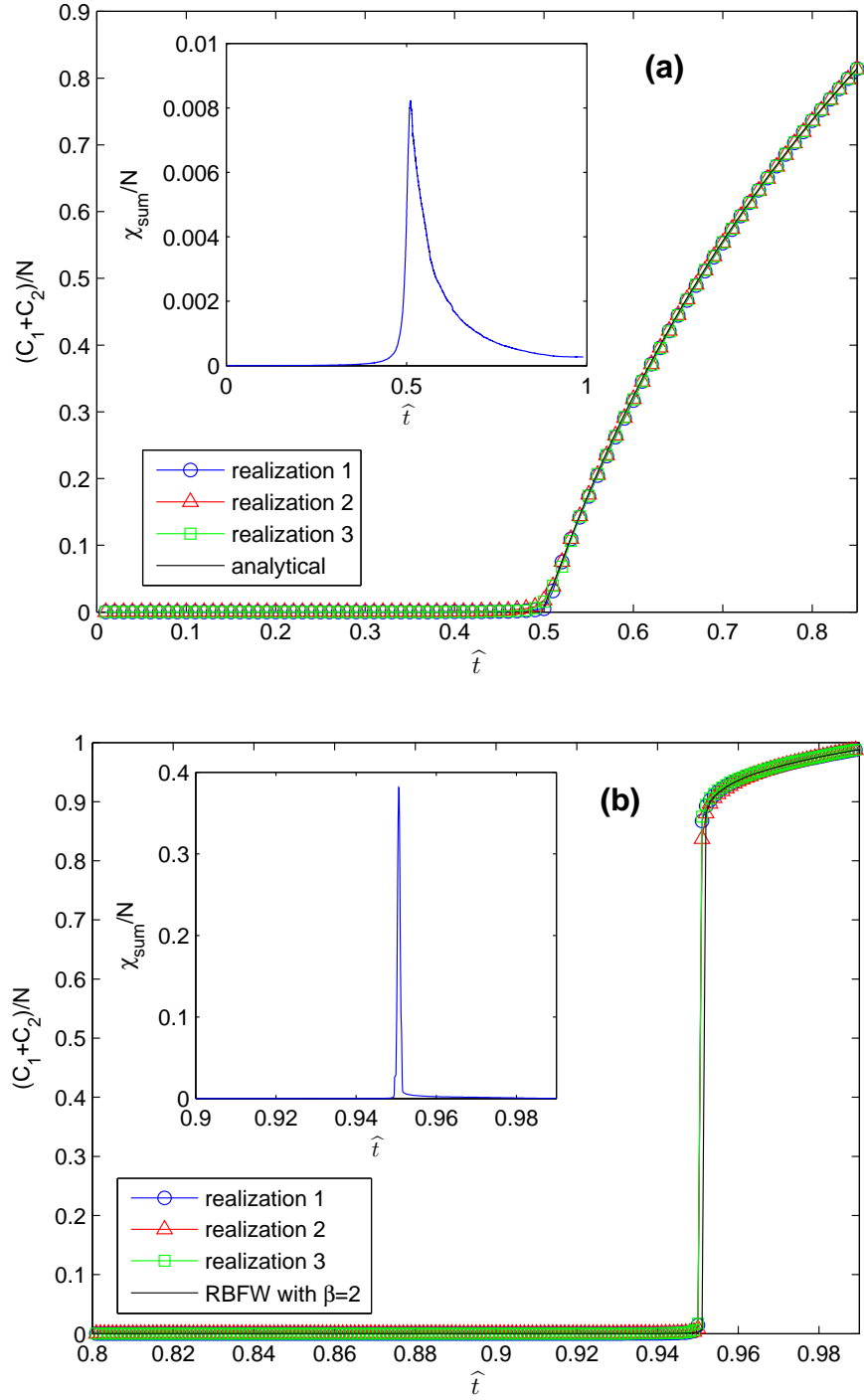
FIG. 10. (Color online) $(C_1 + C_2)/N$ versus $\hat{t}$ (number of external links per node) for the three different realizations in Fig. 7. Inset, the standard deviation of the sum size of giant clusters $\chi_{sum}$ versus $\hat{t}$ over 1000 realizations, $N = 10^6$. (a) multi-ER model. (b) modified BFW model.

$\Delta C_1/\Delta C_2 = C_1/C_2$. In this mode, $C_1(t + \Delta t)/C_2(t + \Delta t) = C_1(t)/C_2(t)$ in expected. Since beyond the critical window all other clusters are much smaller than the two giant ones, the deviation of the ratio $C_1/C_2$ in one step is negligible. Thus after some fluctuation in the critical window, $C_1/C_2$ becomes invariant later in the evolution. In the inset of Fig. 7, the ratios for the three realizations are shown respectively. We can see, $C_1/C_2$ indeed stabilizes to a constant for each realization, but the stable values are different due to the fluctuations in the critical window.

Mode 2. $\Delta C_1/\Delta C_2 = 0$. As in modified BFW model, when the probability of sampling internal-cluster links is larger than $g(k)$, all links that lead to a cluster of size larger than $k$ are always rejected. In this mode, the direct growth of $\mathbf{C_1}$ doesn't work, $C_1$ stays invariant after the transition, and only $C_2$ grows in the following evolution, which can be seen in Fig. 10. Like the different $C_1/C_2$ in multi-ER model, the invariant size $C_1$ is nondeterministic due to the fluctuations in the critical window.

Mode 3. $0 < \Delta C_1/\Delta C_2 < C_1/C_2$. In this case, both $\mathbf{C_1}$ and $\mathbf{C_2}$ grow, but the ratio $C_1/C_2$ decreases in the evolution. In fact, we don't find natural models belonging to this mode.

By the above discussion, we find the behavior in the critical window is crucial for the process, which determines the initial size of different giant clusters and even the evolution later. Especially, in spite of large fluctuations, we can always determine the size $C_1/N$, $C_2/N$ versus $t$ in a given realization, if we know $C_1$, $C_2$ just beyond the critical window. Let's take multi-ER model and BFW model as examples.

In multi-ER model, denote $m = C_1/C_2$ in one realization, which is a constant beyond the critical window according to our analysis. Then in this realization, the system has $\frac{C_1^2 + C_2^2}{(C_1 + C_2)^2} = \frac{m^2 + 1}{(m+1)^2}$ proportion of internal-cluster links compared to a classical ER network with the giant cluster of size $C_1 + C_2$, since the links between $\mathbf{C_1}$ and $\mathbf{C_2}$ are no more internal links. Thus, using the symbols in (11) and (13), the number of all the occupied links is,

$$t = \hat{t} + (\frac{c}{2} - \hat{t})\frac{m^2 + 1}{(m+1)^2}. \tag{15}$$

Combing with (14), we have

$$1 - \gamma = e^{-\frac{2[(m+1)^2 t - 2m\gamma]\gamma}{m^2 + 1 + 2m(1-\gamma)^2}}. \tag{16}$$

Solving (16), we can get $\gamma = (C_1 + C_2)/N$ at time $t$. $C_1/N = \frac{m}{m+1}\gamma$, $C_2/N = \frac{1}{m+1}\gamma$. In the realization 1 in Figure 7(a), $m$ stabilizes at 2.417. The analytical calculation fits the
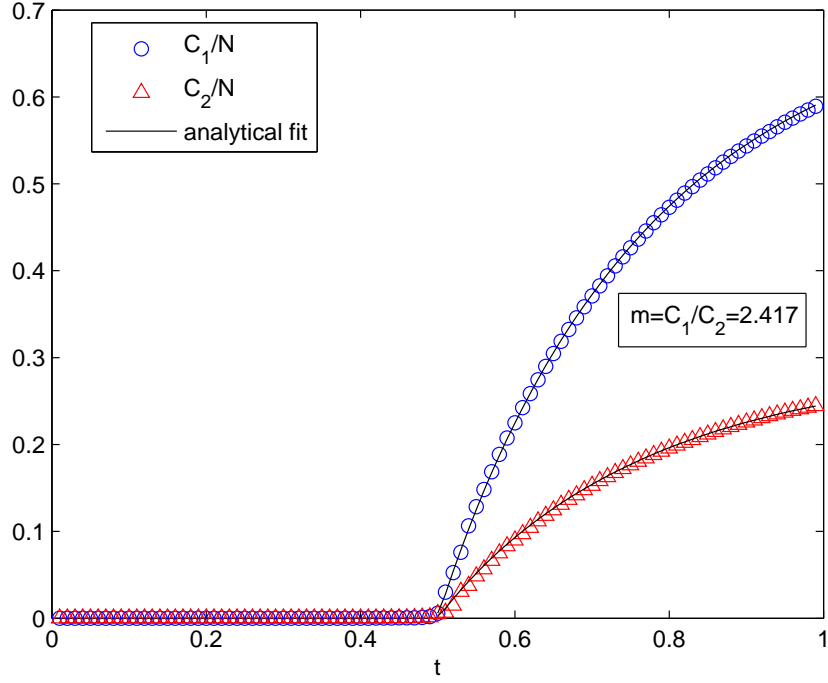
FIG. 11. (Color online) Analytical fit of $C_1/N$, $C_2/N$ in realization 1 in Figure 7(a).

numerical results of this realization very well, which is shown in Fig. 11.

In BFW and modified BFW model, $\mathbf{C_1}$ can be viewed as being frozen, and we can recognize that there is only one giant cluster $\mathbf{C_2}$ in the system. As we have known, the evolution of the sum size $C_1 + C_2$ versus $\hat{t}$ is determined, when internal links are not considered. Having $C_1$, $C_2$ just after transition, we can get the number of internal links in the system and thus determine the two giant clusters sizes versus $t$ in the later evolution of the process. The detail discussion is omitted here.

The analysis above indicates that the fluctuations of size $C_1$ and $C_2$ are mainly due to the stochastic behavior in the critical window, of which the influence is propagated to the later evolution in the process.

## CONCLUSION

In summary, we study how multiple giant clusters could emerge in generic percolation processes on the random network, and show the merging of largest clusters is the only mechanism which prevents the formation of multiple giant clusters. Thus controlling the merging prob-

ability of largest clusters is the key for the emergence of multiple giants, especially we have got the sufficient condition of $k$ stable giant clusters as $\sum_{i,j \leq k, i < j} P_t(\mathbf{C_i}, \mathbf{C_j}) \sim o(1/C_k(t))$ for every $t$. It seems that the emergence of multiple giant clusters is independent to the nature of percolation transition, as we give examples for both discontinuous and continuous transition cases. Our analysis provides insight on the essence of multiple giant clusters in the percolation processes. What's more, multiple giant clusters can be generated in any model of percolation process simply by following our condition, which may have many applications such as, creating communication networks consisting of multiple large clusters operating on different frequencies, or analyzing epidemic infections simultaneously arising in distinct, independent groups.

Unlike the unique giant cluster, large fluctuations in different realizations are observed in the size of multiple giant clusters in many models, which is unanticipated. But without considering the internal links, the sum of all giant clusters sizes shows nearly no fluctuation as the sums in different realizations collapse to the same value. Besides, in every realization, by discussing the relation of the growth of different giant clusters, we show that the early behavior after the transition determines the later evolution, thus the fluctuations are mainly due to the stochastic behavior in the critical window.

Not all percolation processes with multiple giant clusters show large fluctuations in different realizations, for example, the original BFW model. It would be interesting to understand the mechanisms which lead to no fluctuation. Furthermore, a recent work studying the BFW model on the lattice shows no multiple stable giant clusters can coexist on the 2D square lattice [32], which provides a challenge that the emergence of multiple stable giant clusters in various structures of different dimensions should be considered later.

**ACKNOWLEDGMENT**

# REFERENCE

[1] D. Stauffer and A. Aharony, *Introduction to Percolation Theory* (Taylor & Francis, London, 1994).

[2] M. Sahimi, *Applications of Percolation Theory* (Taylor & Francis, London, 1994).

[3] P. Erdös and A. Rényi, Publ. Math. Hugar. Acad. Sci. **5**, 17 (1960).

[4] S. N. Dorogovtsev, J. F. F. Mendes and A. N. Samukhin, Phys. Rev. E **64**, 025101(R) (2001).

[5] J. D. Noh, Phys. Rev. E **76**, 026116 (2007).

[6] Y. Berchenko, Y. Artzy-Randrup, M. Teicher and L. Stone Phys. Rev. Lett. **102**, 138701 (2009).

[7] D. Achlioptas, R. M. D'Souza, and J. Spencer, Science **323**, 1453 (2009).

[8] Y. S. Cho, J. S. Kim, J. Park, B. Kahng, and D. Kim, Phys. Rev. Lett. **103**, 135702 (2009).

[9] F. Radicchi and S. Fortunato, Phys. Rev. Lett. **103**, 168701 (2009).

[10] R. M. Ziff, Phys. Rev. Lett. **103**, 045701 (2009).

[11] R. M. Ziff, Phys. Rev. E **82**, 051105 (2010).

[12] H. Chae, S. H. Yook, and Y. Kim, Phys. Rev. E **85**, 051118 (2012).

[13] N. A. M. Araújo, J. S. Andrade Jr., R. M. Ziff, and H. J. Herrmann, Phys. Rev. Lett. **106**, 095703 (2011).

[14] J. S. Andrade Jr., H. J. Herrmann, A. A. Moreira, and C. L. N. Oliveira, Phys. Rev. E **83**, 031133 (2011).

[15] Y. S. Cho, B. Kahng, and D. Kim, Phys. Rev. E **81**, 030103(R) (2010).

[16] Y. S. Cho and B. Kahng, Phys. Rev. E **84**, 050102(R) (2011).

[17] S. S. Manna and A. Chatterjee, Physica A **390**, 177 (2011).

[18] N. A. M. Araújo and H. J. Herrmann, Phys. Rev. Lett. **105**, 035701 (2010).

[19] K. J. Schrenk, N. A. M. Araújo, and H. J. Herrmann, Phys. Rev. E **84**, 041136 (2011).

[20] A. A. Moreira, E. A. Oliveira, S. D. S. Reis, H. J. Herrmann, and J. S. Andrade Jr., Phys. Rev. E **81**, 040101(R) (2010).

[21] E. J. Friedman and A. S. Landsberg, Phys. Rev. Lett. **103**, 255701 (2009).

[22] R. A. da Costa, S. N. Dorogovtsev, A. V. Goltsev, and J. F. F. Mendes, Phys. Rev. Lett. **105**, 255701 (2010).

[23] P. Grassberger, C. Christensen, G. Bizhani, S.-W. Son, and M. Paczuski, Phys. Rev. Lett. **106**, 225701 (2011).

[24] H. K. Lee, B. J. Kim, and H. Park, Phys. Rev. E **84**, 020101(R) (2011).

[25] L. Tian and D.-N. Shi, Phys. Lett. A **376**, 286 (2012).

[26] O. Riordan and L. Warnke, Science **333**, 322 (2011).

[27] J. Nagler, A. Levina and M. Timme, Nature Phys. **7**, 265 (2011).

[28] H. D. Rozenfeld, L. K. Gallos, and H. A. Makse, Eur. Phys. J. B **75**, 305 (2010).

[29] T. Bohman, A. Frieze, and N. C. Wormald, Random Struct. Algorithms **25**, 432 (2004).

[30] W. Chen and R. M. D'Souza, Phys. Rev. Lett. **106**, 115701 (2011).

[31] E. Ben-Naim and P. L. Krapivsky, J. Phys. A **38**, L417 (2005).

[32] K. J. Schrenk, A. Felder, S. Deflorin, N. A. M. Araújo, R. M. D'Souza, and H. J. Herrmann, Phys. Rev. E **85**, 031103 (2012).

[33] R. M. D'Souza and M. Mitzenmacher, Phys. Rev. Lett. **104**, 195702 (2010).

[34] S. D. S. Reis, A. A. Moreira, and J. S. Andrade Jr., Phys. Rev. E **85**, 041112 (2012).

[35] P.-S. Shim, H. K. Lee, and J. D. Noh, Phys. Rev. E **86**, 031113 (2012).

[36] B. Bollobás, *Random Graphs*, 2nd ed. (Cambridge University Press, 2001).

[37] M. E. J. Newman, S. H. Strogatz, and D. J. Watts, Phys. Rev. E **64**, 026118 (2001).

[38] W. Chen and R. M. D'Souza, e-print arXiv:1106.2088.

[39] O. Riordan and L. Warnke, Phys. Rev. E **86**, 011129 (2012).

[40] S. Janson, T. Łuczak, and A. Rucinski, *Random Graphs*, (John Wiley & Sons, 2000).